Available online at www.sciencedirect.com
SCIENCE DIRECT®
Journal of Power Sources 142 (2005) 243–252
JOURNAL OF POWER SOURCES
www.elsevier.com/locate/jpowsour

The electrochemical characteristics of air fuel cell electrodes used in an electrolytic system for spent chromium plating solution regeneration

Kuo-Lin Huang[a,*], Thomas M. Holsen[b], J.R. Selman[c], Tse-Chuan Chou[d]

[a] *Department of Environmental Engineering and Science, National Pingtung University of Science and Technology, Neipu, Pingtung 91201, Taiwan*
[b] *Department of Civil and Environmental Engineering, Clarkson University, Potsdam, NY 13699, USA*
[c] *Department of Chemical and Environmental Engineering, Illinois Institute of Technology, Chicago, IL 60616, USA*
[d] *Department of Chemical Engineering, National Cheng Kung University, Tainan 70101, Taiwan*

Received 15 September 2004; received in revised form 30 September 2004; accepted 30 September 2004
Available online 21 December 2004

Abstract

The electrochemical characteristics of lab prepared Pt|Nafion and commercial Pt–C|Nafion air fuel cell electrodes in sulfuric and chromic acid electrolytes were examined to help in the design of an electrochemical system that might potentially be used in the regeneration of spent chromium plating solutions to save energy. In both solutions, the Pt–C|Nafion electrode obtained higher cathodic currents from oxygen reduction than the Pt|Nafion electrode, mainly due to an order of magnitude greater active area in the Pt–C|Nafion than in the Pt|Nafion electrode. The currents significantly increased after the cathodic sweeps passed ∼0.7–0.8 V versus a standard hydrogen electrode (SHE) in both systems. The currents for the oxygen reduction reactions were higher in the sulfuric acid system than in the chromic acid system, which were associated with less available electroactive sites on the electrodes and/or the inhibition of oxygen reduction in the chromic acid. In addition, impurities (i.e., Cu) were more difficult to deposit on Pt in the chromic acid than in the sulfuric acid. In sulfuric acid, the Tafel slopes were similar for the two electrodes, but in chromic acid, the Pt–C|Nafion electrode had a Tafel slope close to $-120\,\text{mV decade}^{-1}$ while the Pt|Nafion did not have a clear Tafel region in ∼600–400 mV versus Ag/AgCl. The polarization results suggest that, in practical applications, flooding, if it occurs, will be more responsible than slow oxygen reduction kinetics for the cathodic potential/cell voltage increase in the fuel cell cathode system using chromic acid.

Keywords: Electrochemical characteristics; Fuel cell electrodes; Oxygen reduction; Chromium plating solutions

1. Introduction

The ability of polymer-electrolyte fuel cells (PEFCs) to produce energy has been investigated for several decades. The cells were initially used in spacecraft and are currently being investigated for use in electric vehicles. PEFCs have high power densities, are compact, generally do not leak electrolyte, and are stable at room temperature [1].

One type of PEFCs is the hydrogen–oxygen fuel cell that generally consists of a membrane electrode assembly (MEA) and two graphite plates with a gas inlet and outlet. Hydrogen oxidation and oxygen reduction occur at the anode and cathode, respectively, which are placed at opposite sides of the MEA. Its performance is controlled by the slow kinetics of oxygen reduction at the O_2 side of MEA [2].

A commercial MEA (ElectroChem Inc.) commonly includes the components of carbon paper/cloth, platinum–carbon (Pt–C) mixture, and Nafion® membrane [1,3]. The Pt–C mixture is comprised of fine platinum grains supported by larger carbon powder with a porous carbon fiber backing which allows air to pass through [1,4]. One side of the

* Corresponding author. Tel.: +886 8 770 3202x7092; fax: +886 8 774 0256.
E-mail address: huangkl@mail.npust.edu.tw (K.-L. Huang).

0378-7753/$ – see front matter © 2004 Elsevier B.V. All rights reserved.
doi:10.1016/j.jpowsour.2004.09.040

commercial MEA can be used as a Pt–C catalyst cathode with a three-dimensional reaction region that is similar to a three-dimensional cathode that has been used extensively in industrial electrowinning [5]. This design improves the rates of electrochemical reactions of interest on the cathode over a conventional planar electrode.

In hard chromium plating, a process widely used in chromium electroplating industry, the buildup of impurities (i.e., Cu(II), Ni(II), and Fe(III) from raw materials and Cr(III) from Cr(VI) reduction on cathodes) limits the lifetime of the plating solutions because their presence degrades the quality of the chromium deposit [6]. Since the disposal of spent chromic acid containing very high concentrations of toxic Cr(VI) is expensive and can cause significant environmental degradation, there is increasing interest in finding ways to regenerate waste chromium liquors [7].

Electrolytic separation is one of the techniques currently employed for the regeneration of spent chromium plating solutions [6–8]. This process, mainly influenced by electrode materials, electrolytes, separators, and operational parameters (currents/potentials), is not very well understood because the metal impurities (i.e., Cr(III) and Fe(II)) oxidation/O_2 evolution and metal ion impurities reduction/H_2 evolution that occur at the anode and cathode, respectively, are complicated.

An electrolytic cell separated by a ceramic diaphragm [6,8] or a Nafion membrane can simultaneously oxidize Cr(III) to Cr(VI) on the anode and transport metal ion impurities from the anolyte to the catholyte to regenerate chromium plating solutions [7]. In these processes the anodic oxidation of Cr(III) to Cr(VI) is, in general, of minor concern because it is much faster than the transport of the other impurities through the separator. In addition, although the separator-phase diffusivities and mobilities of Cu(II), Ni(II), and Fe(III) are greater in a ceramic than in a Nafion membrane, the transport of these impurities through the ceramic may be much slower than through the Nafion membrane because the ceramic is much thicker [7].

Collecting solutions (catholytes) may also influence impurity removal. Metal hydroxide sludge can deposit on the cathode, accumulate in a sulfuric acid catholyte, and clog the ceramic separator, resulting in a rapid increase in cell voltage [6], whereas for a chromic acid catholyte system using both the Nafion membrane and ceramic diaphragm separators, no metal hydroxide sludge was observed [7]. Nevertheless, the process needs fairly high power requirements, especially when impurity metal compounds coat the cathodes. For this process, therefore, another area of research is on how to lower the power requirements.

The air cathode used in H_2–O_2/air fuel cell systems (instead of hydrogen evolving cathodes) may potentially be applied to an electrolytic system for spent chromium plating solution regeneration to improve its efficiency and lower its power requirement [4]. An in-house Pt–C|Nafion air fuel cell cathode was first tested by Ahmed et al. [4] in an electrochemical membrane process to remove contaminants from hard chromium electroplating solutions and to determine if the use of a fuel cell cathode could save cell voltage (energy). Although no direct comparison was made with the existing commercial process involving a porous diaphragm, they compared cell voltage for an air-fed MEA with that for a nitrogen-fed one (in which hydrogen evolution occurred). They found that the required cell voltage was lowered (at constant current) when the nitrogen gas was replaced with oxygen; however, the cell voltage increased with time. This increase was attributed to flooding of the MEA. Similarly, it is possible that gradual flooding caused the cell voltage increase in a commercial Pt–C|Nafion during ∼4.5 days of operation (particularly within the first 24 h) in our earlier work [9]; it was also found that the system using the Pt–C|Nafion MEA needed approximately 3 V more than that was needed for the system with a Pt|Nafion cathode in operation at constant current [9]. Ahmed et al. [4,10] also indicated that Cu, Fe, Ni, and Cr might deposit on the electrode matrix and deactivate the Pt-catalyst causing a rising cell voltage.

The Pt|Nafion MEA, like a Pt–C|Nafion MEA, is also a three-dimensional electrode [9]. However, its Pt grains penetrate into the Nation solid electrolyte deeper than in a Pt–C|Nafion MEA. There is a trade-off in the designs of these two cathodes for—(i) proton conduction: Pt > Pt–C, (ii) electron conduction: Pt > Pt–C, and (iii) O_2 transfer: Pt < Pt–C for the oxygen reduction in acid electrolytes.

In this work the cathode flooding associated with the cell voltage increase was explored, the electrochemical characteristics of the process, including kinetic parameters of oxygen reduction of the commercial Pt–C|Nafion MEA and the Pt|Nafion MEA were determined and their operational characteristics were compared. In addition, both sulfuric and chromic acid, as possible catholytes were compared. Finally, due to a concern that the deposition of catholyte impurity (i.e., Cu(II)) might deteriorate the performance of the air fuel cell cathode, a planar Pt electrode was used in cyclic voltammetry to determine if the chromic acid catholyte impurities (Cu(II)) was deposited on the Pt surface.

2. Experimental

The cathodic half cell of a previously employed two-compartment cell made of acrylic plastic [9] was used in the experiments. It included an electrolyte compartment, MEA, Pt gauze (current conductor), graphite plate (current conductor and support) with air inlet and outlet, copper foil (current collector), gasket, and acrylic holder (Fig. 1a). Screws and nuts connected the electrolyte compartment and the air fuel cell cathode assembly.

The effective projected areas of the MEAs were 5 cm^2. The Pt–C|Nafion MEA (FC05-MEA, 1 mg cm^{-2} Pt loading, 20 wt.% Pt–C), Pt gauze, and graphite plate (FC05-MP) were purchased from ElectroChem Inc. (Woburn, MA). The Pt|Nafion MEA was made by the impregnation-reduction (I-R) method [11–14] which is briefly described here. An acid

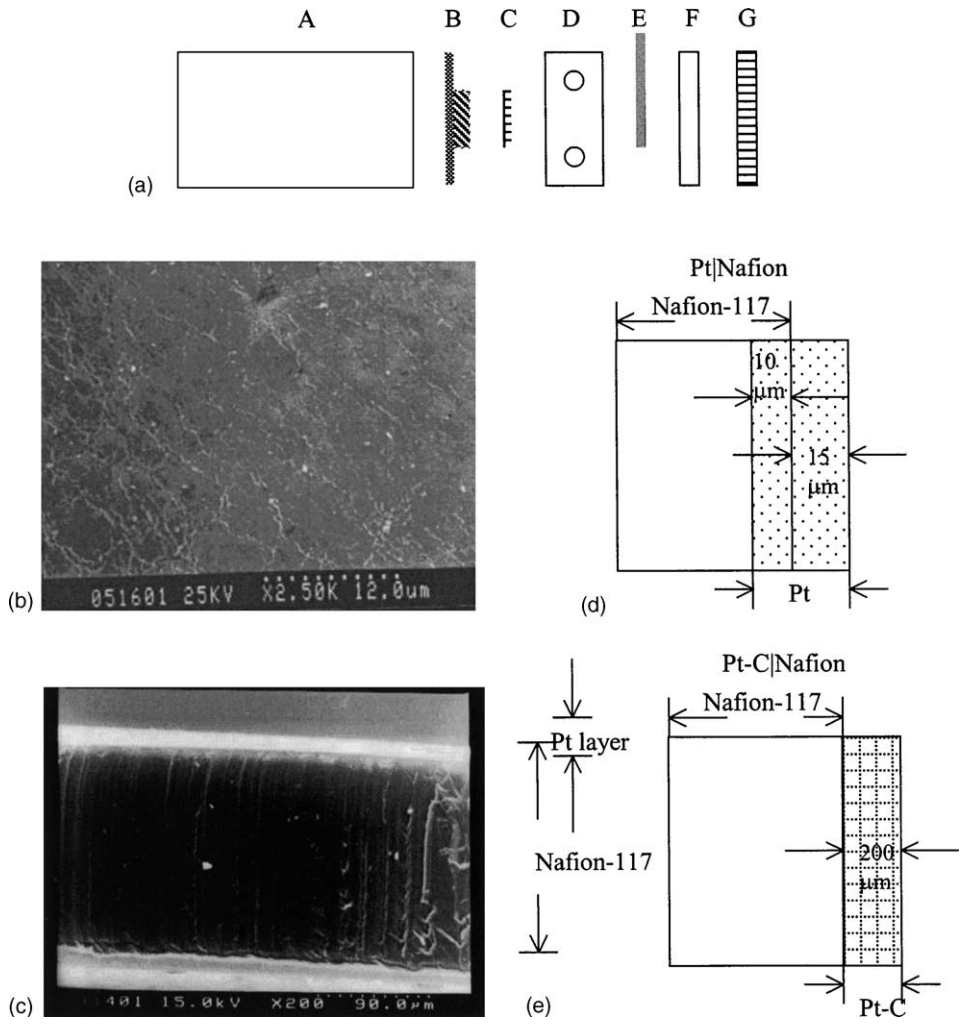

Fig. 1. (a) Schematic diagram of each unit that was assembled for the experimental cell (A: electrolyte compartment, B: MEA, C: Pt gauze, D: graphite plate, E: Cu foil, F: silicon gasket, and G: acrylic holder); (b) Pt|Nafion SEM photo (top-view); (c) Pt|Nafion SEM photo (side-view) (from [9] with the permission of Selper Ltd. and Environmental Technology); (d) Pt|Nafion; and (e) Pt–C|Nafion.

cleaned Nation membrane was soaked in a 0.01 M platinum tetramine ($Pt(NH3)_4Cl_2$, 99%, Stern Chemicals) solution before it was washed with deionized water and immersed in a 0.1 M NaBHU (95%, Ferak) reducing solution for 2 h. It was then equilibrated in a 2 M sulfuric acid solution followed by pure water cleaning to remove impurities. After this treatment, the Pt particles covered the surface of one side of the Nafion piece with a thickness of about 15 μm at a Pt loading of 1.35 mg cm^{-2}. The Pt particles penetrated into the Nafion to a depth of ∼10 μm (Fig. 1b–d) [9]. The Pt–C piece of the commercial Pt–C|Nafion had a measured thickness of ∼200 μm (Fig. 1e).

The 2 M sulfuric acid solution was prepared by diluting a concentrated sulfuric acid (96–98%, trace metal grade, RDH) with deionized water (>18.3 MΩ cm) while the chromic acid was prepared from dissolving CrO_3 (99.9%, Aldrich) in deionized water. Two 0.1 M $CuSO_4$ (99.99%, Aldrich) solutions (in 2 M H_2SO_4 and 2.12 M CrO_3) were used in a cyclic voltammetric experiment to investigate the oxidation/reduction of Cu(II)/Cu on a planar Pt electrode.

The cathode-fed gases were N_2, air, or O_2 supplied at a flowrate of 100 cm^3 min^{-1} for cyclic and linear scanning voltammetric tests. The supporting electrolyte was either 2 M sulfuric acid or 2.12 M chromic acid solution with a volume of 300 mL. The electrolytes were purged with purified nitrogen gas (∼100 cm^3 min^{-1}) during and before each experiment. The electrochemical tests were performed using an EG&G potentiostat (Model 263A). Cyclic sweeps continued for about 400 cycles (about 60 min) (scan rate 100 mV s^{-1}) until stable cyclic voltammograms were obtained. Slow linear sweeps at 1 mV s^{-1} (pseudo-steady-state) were used to simulate steady-state polarization. In the initial experiments, the linear sweeps resulting from 1 to 0.5 mV s^{-1} rates were found to be nearly identical so a scan rate of 1 mV s^{-1} was used for the remainder of the experiments.

The potentials reported were all versus Ag/AgCl, except cell voltages. The Ag/AgCl reference electrode and a platinum counter electrode were located in the sulfuric or chromic acid solution in the electrolyte compartment. All the experiments were performed at room temperature.

3. Results and discussion

3.1. Cyclic voltammograms (CVs)

3.1.1. Pt–C|Nafion MEA

The CVs obtained at the MEA's Pt–C|Nafion interface in both sulfuric and chromic acids were similar (Fig. 2(a) and (b)). When nitrogen was used, hydrogen adsorption (A in Fig. 2(a)) and desorption (B in Fig. 2(a)) can be seen. At potentials of around 1000–1100 mV, the measured current became negative and oxygen underwent a 4-electron reduction (Reaction (1)) [15–16]. Yeager [15] indicated that this reaction occurs predominantly in acid electrolytes with air cathodes containing very highly dispersed Pt on a moderately high surface area carbon support. In a properly working MEA with good gas access, the 4-electron reaction would presumably dominate because overpotentials would remain modest. With further cathodic sweeps, a 2-electron reduction of O_2 to peroxide (Reaction (2)) [15] accompanied by Pt oxide reduction would probably occur around potentials of 400–500 mV. Under more negative cathodic sweeps at potentials of about −200 mV, hydrogen evolution appears.

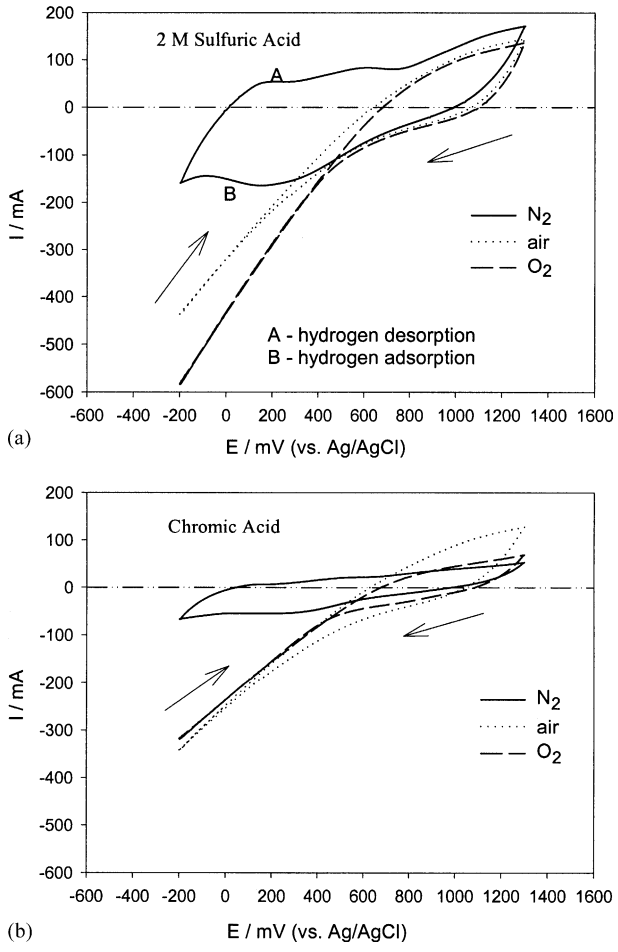

Fig. 2. CVs of Pt–C|Nafion electrode in (a) 2 M sulfuric acid and (b) 2.12 M chromic acid using N_2, air, and O_2 electrode feeding gases. Scan rate = 100 mV s^{-1}; beginning point: −200 mV vs. Ag/AgCl.

$$O_2 + 4H^+ + 4e^- = 2H_2O; \quad E^0 = 1.229\,\text{V (versus SHE)} \tag{1}$$

$$O_2 + 2H^+ + 2e^- = H_2O_2; \quad E^0 = 0.670\,\text{V (versus SHE)} \tag{2}$$

For the carbon supported Pt|Nafion MEA, carbon is not an effective catalyst for O_2 reduction by either the direct 4-electron pathway or the peroxide formation pathway in acid electrolyte [15].

The CVs using air and oxygen as feed gases were quite similar in both acids and very different than those obtained using nitrogen. Using the Pt–C|Nafion MEA in H_2SO_4, there was about a 180 mV potential difference between air and oxygen at 400 mA (80 mA cm^{-2}) cathodic current. This was far more than the thermodynamically expected difference of 10–11 mV ((*RT*/4*F*)(ln(l.0/0.21)) = 15 mV decade^{-1} of O_2 pressure) [2]. This difference means that there was significant polarization resistance (and/or perhaps ohmic resistance) increasing approximately linearly with current density in this MEA. This occurred far more for air than for oxygen. In other words, gas phase diffusion resistance was dominant. On a SHE scale, the values of the electrode potential at this current density were as follows: +20 mV for oxygen, −170 mV for air, −400 mV for hydrogen evolution.

At the same current density in H_2CrO_4, the same MEA, when fed with air or oxygen had a much smaller potential difference, in fact close to the thermodynamic value. This implies that the polarization resistance and ohmic resistance were about the same for oxygen and air. However, the electrode potentials in H_2CrO_4 were far more negative than in H_2SO_4, for example, at 400 mA, approximately −300 mV for both oxygen and air. Hydrogen evolution appeared to require approximately −500 mV. This huge overpotential for oxygen and air (1500 mV) suggests that the MEA was probably flooded, or alternatively the kinetic for oxygen reduction were very slow, or both. The overpotential for hydrogen evolution was also large (−500 mV), but not much more than that in H_2SO_4 (−400 mV).

3.1.2. Impregnation-reduction Pt|Nafion electrode

In a sulfuric acid solution, the CV of the Pt|Nafion electrode was similar to that measured using a common planar Pt electrode (Fig. 3(a)). The peaks indicating hydrogen adsorption (A in Fig. 3(a))/desorption (B in Fig. 3(a)) were clearly detected. Comparing the CVs of the two different MEAs during the feeding of N_2 gas within the potential range of −200 to 200 mV (Figs. 2(a) and 3(a)), the Pt–C|Nafion type MEA had higher scan areas for hydrogen adsorption and desorption indicating it had a larger electroactive Pt area. The typical Pt oxidation plateau (C in Fig. 3(a)) and the reduction peak of Pt oxides (D in Fig. 3(a)) were also clearly detected.

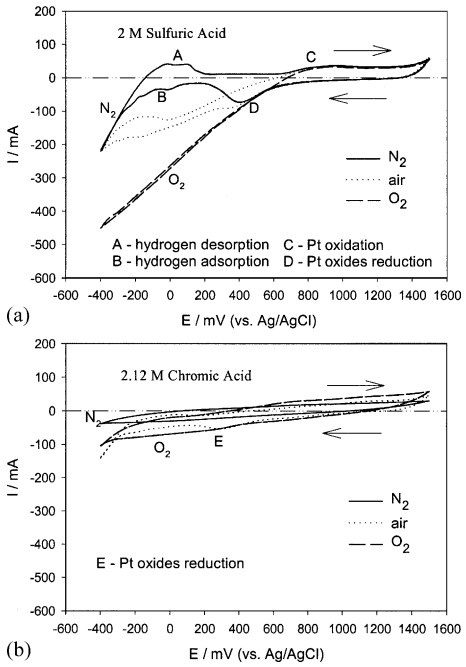

Fig. 3. CVs of Pt|Nafion electrode in (a) 2 M sulfuric acid and (b) 2.12 M chromic acid using N_2, air and O_2 electrode feeding gases. Scan rate = 100 mV s^{-1}; beginning point: −400 mV vs. Ag/AgCl.

During feeding of the electrodes with air, the cyclic sweeps of the Pt|Nafion electrode in both sulfuric and chromic acids showed Pt oxide reduction peaks (D in Fig. 3(a) and E in Fig. 3(b), respectively), which indicates that the rate of oxygen reduction decreased when the impregnation-reduction type Pt|Nafion electrode was used over what occurred using the Pt–C|Nafion electrode. This was probably because the Pt–C electrode incorporating carbon paper and particle supported Pt had larger voids than the Pt grains of the Pt|Nafion electrode allowing better oxygen transfer.

When comparing the performance of the Pt|Nafion MEA in H_2SO_4 and H_2CrO_4 at the same current density (80 mA cm^{-2}) (Fig. 3), a 270 mV potential difference between air and oxygen in H_2SO_4 (i.e., a 50% increased potential difference compared to the Pt–C|Nafion MEA) was measured. The electrode potential for oxygen at that current density was −200 mV versus Ag/AgCl (i.e., 220 mV more negative than for the Pt–C|Nafion MEA). This finding also implies that the active area in this MEA was far smaller than for the Pt–C|Nafion MEA, by almost an order of magnitude (assuming the Tafel slope should be 120 mV per decade for high-rate oxygen reduction). The 270 mV difference between air and oxygen strongly suggests flooding occurred. In H_2CrO_4 there was again little difference between air and oxygen, similar to the case for the Pt–C|Nafion MEA. However, the value of the electrode potential was approximately 280 mV more negative than with the Pt–C|Nafion MEA. This finding confirmed the inference from the H_2SO_4 measurements, that the Pt|Nafion MEA, in addition to being flooded, had a far smaller active area than the Pt–C|Nafion MEA.

The oxygen diffusion resistance in the Pt catalyst layer of Pt|Nafion cathode should be greater than that in the Pt–C catalyst mixture of Pt–C|Nafion cathode. The catalyst Pt particles in the Pt–C not in direct contact with Nafion can also be involved in interfacial electrochemical reactions (i.e., O_2 reduction) and contribute to cyclic voltammograms mainly through the pathway of surface conductance on carbon particles with a significant ohmic drop effect [17]. Consequently, the ohmic drop is inherently larger in the Pt–C piece of Pt–C|Nafion than in the Pt layer of Pt|Nafion. If electrolyte entered the pores of MEAs, more electrolyte will be retained in the more porous Pt–C than in Pt, thus increasing the flooding and cause a need for greater cell voltage.

3.2. Linear sweep voltammograms (LSVs)

3.2.1. Pt–C|Nafion MEA

The cathodic LSV results using both air and oxygen in both acids were quite similar. In all cases the cathodic current due to oxygen reduction (Reaction (1), on the oxide-covered Pt) obviously increased around a potential of 600 mV (Fig. 4).

For the Pt–C|Nafion cathode in H_2SO_4 the potential difference between air and oxygen was initially small. However, it gradually increased to approximately 11 mV at 20 mA cm^{-2} (100 mA) and to approximately 180 mV at 80 mA cm^{-2} (400 mA). This finding was similar to that found in the CV scans discussed in Section 3.1.1, probably due to ohmic resistance increasing with increasing current density. On the other hand, using the Pt–C|Nafion electrode in H_2CrO_4, the potential difference between air and oxygen over the

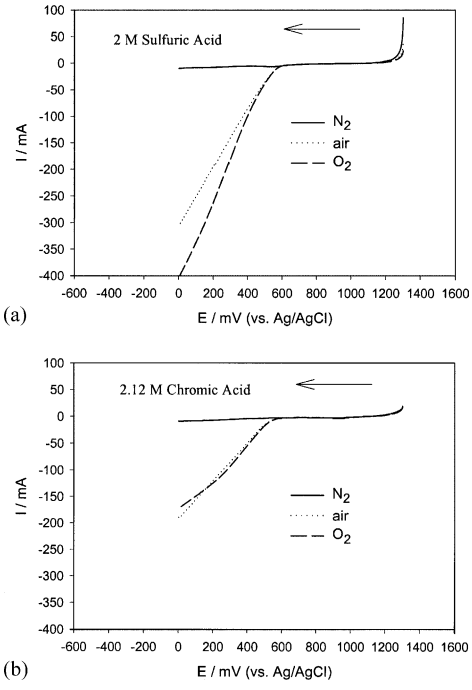

Fig. 4. Cathodic LSVs of Pt–C|Nafion electrode in (a) 2 M sulfuric acid and (b) 2.12 M chromic acid using N_2, air, and O_2 feeding gases. Scan rate: 1 mV s^{-1}; beginning point: +1300 mV vs. Ag/AgCl.

entire cathodic current density range (up to 35 mA cm^{-2}) was small (~11 mV), indicating that under this quasi-steady-state condition the Pt–C MEA was functioning as expected. This finding was also suggested by the relatively low polarization (electrode potentials being above +200 mV versus SHE). However, the currents obtained were smaller than those in H_2SO_4 (i.e., approximately one-half smaller for the O_2 case), indicating the possible inhibition of oxygen reduction in H_2CrO_4. This inhibition was also reflected in the overpotential of 1600 mV.

3.2.2. Impregnation-reduction Pt|Nafion MEA

Similar results were also observed when comparing the cathodic LSVs of the Pt|Nafion electrode in the sulfuric acid and chromic acid solutions (Fig. 5(a) and (b), respectively), i.e., apparent current increase of around 600 mV during air and O_2 feeding, greater potential difference between air and oxygen in sulfuric acid than in chromic acid, and greater cathodic current using air and oxygen in sulfuric acid than in chromic acid. The corresponding currents in sulfuric acid and chromic acid were smaller using the Pt|Nafion electrode than using the Pt–C|Nafion electrode confirming that the former electrode had a smaller active area than the latter. This was also supported by comparing their CVs during N_2 feeding for hydrogen adsorption and desorption (Figs. 2 and 3). The increased currents were also possibly due to the fact that the Pt–C|Nafion had a higher O_2 transfer rate and/or a better dispersed Pt catalyst resulting in more active sites than for the Pt|Nafion MEA.

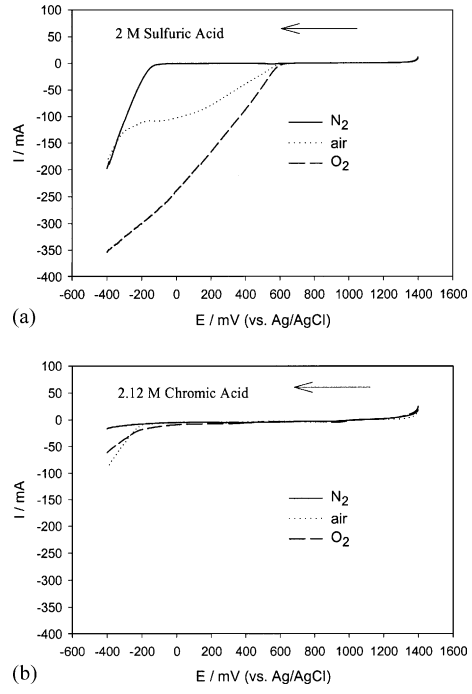

Fig. 5. Cathodic LSVs of Pt|Nafion electrode in (a) 2 M sulfuric acid and (b) 2.12 M chromic acid using N_2, air, and O_2 feeding gases. Scan rate = 1 mV s^{-1}; beginning point: +1400 mV vs. Ag/AgCl.

Interestingly, H_2 evolution began around −200 mV (close to 0 mV versus SHE) for all the three gases in both acids using the Pt|Nafion, revealing that the electrode worked as expected for H_2 evolution in both low pH solutions. Therefore, for both the MEAs, the smaller current density obtained in the chromic acid solution than in the sulfuric acid solution should be mostly attributed to the effect of using different electrolytes.

3.2.3. Tafel plots

In the sulfuric acid solution, a two-slope Tafel region was observed for both the Pt–C|Nafion and Pt|Nafion (Figs. 6(a) and 7(a), respectively) in the 400–800 mV versus Ag/AgCl range, indicating a mixed ohmic-kinetic control [10]. However, when the potential was smaller than 400 mV versus Ag/AgCl, the slope increased again and the curves suggest there was a mass transfer controlled region.

The Tafel slope for the oxygen reduction reaction on the Pt–C|Nafion in the sulfuric acid solution was close to −120 mV decade^{-1} and it was approximately three times that in the high and low current density regions, respectively (Fig. 6(a)). This was somewhat similar to that for the Pt|Nafion having a narrow current density (log(*i*)) range (−2.6 to −2.1 A cm^{-2}) for the slope of −120 mV decade^{-1} and a three times higher slope in the high and low

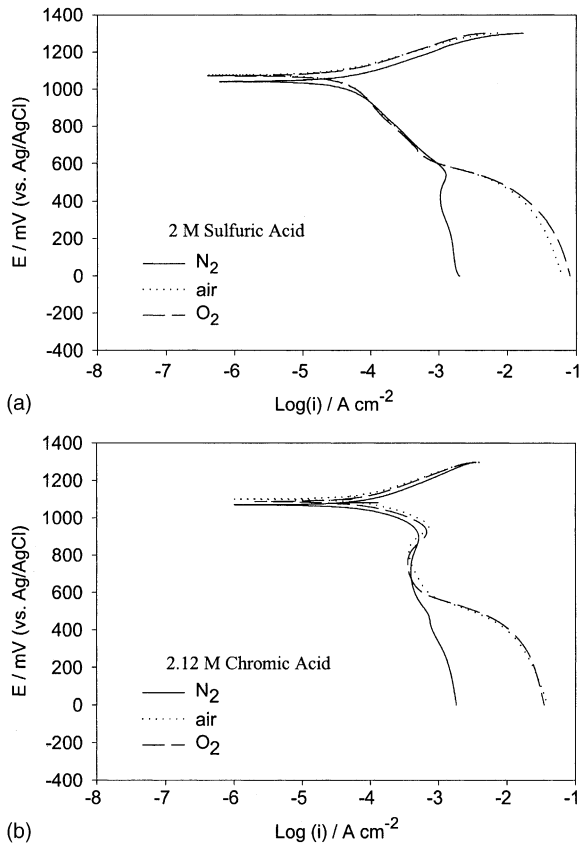

Fig. 6. *E*–log(*i*) plots of Pt–C|Nafion electrode in (a) 2 M sulfuric acid and (b) 2.12 M chromic acid.

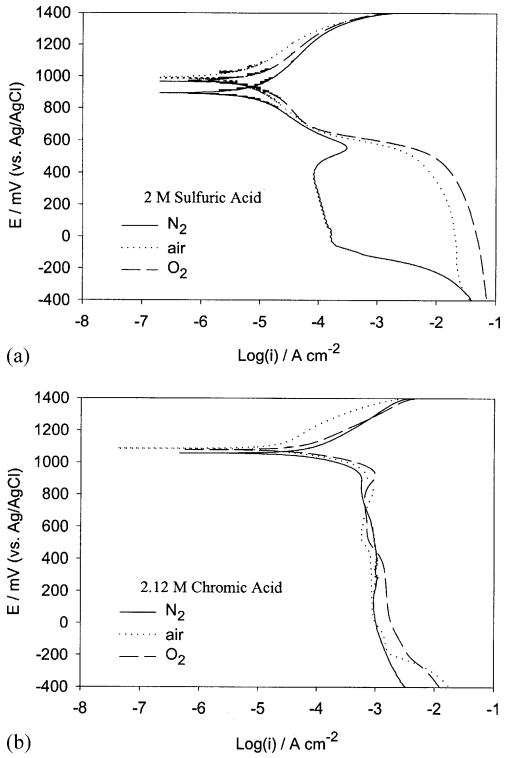

Fig. 7. E–log(i) plots of Pt|Nafion electrode in (a) 2 M sulfuric acid and (b) 2.12 M chromic acid.

current density regions, respectively. The slope was around -60 mV decade^{-1} in a wider high current density region (more than one decade of current density (log(i) = -3.8 to -2.7 A cm^{-2})) (Fig. 7(a)). These slopes in the high and low current density regions correspond to oxygen reduction on oxide-free and oxide-covered Pt, respectively [18]. The oxide-covering on the Pt surface can block oxygen transfer reduction [2] and electron migration or tunneling [19]. Sepa et al. [20] indicated that the Tafel slope for oxygen reduction on Pt in acid or alkaline solutions was -60 mV decade^{-1} in a low potential polarization region. Others have reported that the Tafel slopes of -60 and -120 mV decade^{-1} were common for low and high current density regions, respectively [18–23].

The existence of several Tafel slopes and non-linear Tafel diagrams may be interpreted as (i) the change in Tafel slope from -60 to -120 mV decade^{-1} caused by a kinetic change of oxygen reduction on Pt–C catalyst due to the change of oxygen coverage on Pt surface around 850 mV versus SHE and (ii) the limiting ohmic effect in the catalyst layer and the diffusion limitation in the flooded-agglomerate leading to a doubling of Tafel slopes at high current densities [24].

Unlike the case in sulfuric acid solution, the log(i) in Tafel plot for the Pt–C|Nafion in the chromic acid solution decreased when the potential was lower than 900 mV versus Ag/AgCl and it seemed to be a plateau for each gas around 800–600 mV versus Ag/AgCl (Fig. 6(b)). The trend of log(i) versus E curves for air/O_2 feeding cases was similar to those in sulfuric acid solution at the potential <600 mV versus Ag/AgCl. The negative resistance region was previously reported using a Pt plate as a working electrode in chromic acid solution and is considered to be evidence of the formation of a cathodic film by Hoare [25]. It might also be explained by a superposition of several phenomena (i.e., reactions) occurring in the same range of potential for the non-linear Tafel diagrams [24].

In the same chromic acid solution, the shape of the Tafel plot for the Pt|Nafion (Fig. 7(b)) was fairly similar to that for Pt–C|Nafion. However, the decrease in log(i) was smaller within 800–600 mV versus Ag/AgCl and the increase in log(i) when it is greater than -3 was significantly smaller for the former electrode than for the latter, which was probably due to the much smaller active surface area for the Pt|Nafion electrode. For both electrodes, the -60 and -120 mV decade^{-1} in Tafel slopes were obtained in the low current density region with a narrow potential range around 1080–960 mV versus Ag/AgCl. Nevertheless, the Pt–C|Nafion had a Tafel slope close to -120 mV decade^{-1} between log(i) = -3 to -2 (~600–400 mV versus Ag/AgCl) while the Pt|Nafion did not exhibit a clear Tafel region in that range.

3.3. Comparison of sulfuric and chromic acid catholytes

According to the above comparisons (Figs. 2–7, particularly Figs. 6 and 7), the electrolyte effect on oxygen reduction for both the electrodes was remarkable. The two electrodes obviously gained smaller cathodic current from oxygen reduction in the chromic acid solution than in the sulfuric acid solution; in other words, the electrodes needed more polarization to obtain the same current density of oxygen reduction in the chromic acid solution than in sulfuric acid solution (Table 1). This was possibly due to fewer available electroactive sites because the electrode surface was covered with a cathodic film and/or the inhibition of oxygen reduction in chromic acid at room temperature. The gas-phase oxygen reduction on a Pt electrode was previously reported to be significantly inhibited in the presence of Cr(VI) species (e.g., CrO_3) at high temperature [26]. Therefore, the sulfuric acid solution should be more suitable than the chromic acid solution as a collecting solution (catholyte) when the Pt|Nafion or Pt–C|Nafion cathode is used because a greater system current from oxygen reduction reactions will be obtained at same cathodic potential. Note that the exchange current densities around the apparent equilibrium potential for oxygen reduction did not differ for either electrode or electrolyte. These exchange current densities obtained at pseudo-steady-state using a scan rate of 1 mV s^{-1} were in the 10^{-4} to 10^{-5} A cm^{-2} range, which implies that the kinetics of oxygen reduction for both electrodes were not as poor as expected in the two electrolytes, especially in the chromic acid. In contrast to the oxygen reduction reaction, hydrogen evolution around -200 mV versus Ag/AgCl (0 mV versus SHE) was apparent in each electrolyte (Table 1) because of the abundance of protons and fast kinetics.

Table 1
Standard electrode potentials (vs. SHE) and actual electrode potentials (vs. SHE) for O_2 reduction and H_2 evolution

Standard electrode potentials (V)	Actual O_2 reduction and H_2 evolution electrode potentials[a] (V)			
	Pt–C|Nafion		Pt|Nafion	
	H_2SO_4	H_2CrO_4	H_2SO_4	H_2CrO_4
+1.33 (Cr^{6+}/Cr^{3+}), +1.22 (O_2/H_2O) [O_2 reduction in O_2]	~+0.8 (0.60)[b] [O_2 reduction in O_2]	~+0.8 (0.48)[b] [O_2 reduction in O_2]	~+0.8 (0.57)[b] [O_2 reduction in O_2]	~+0.7 [O_2 reduction in O_2]
+0.67 (O_2/H_2O_2), +0.34 (Cu^{2+}/Cu^0), +0.197 RE [Ag/AgCl]				
0 (H^+/H_2) [H_2 evolution]: −0.23 (Ni^{2+}/Ni^0), −0.409 (Fe^{2+}/Fe^0), −0.41 (Cr^{3+}/Cr^{2+}), −0.557 (Cr^{2+}/Cr^0)	~0[c] [H_2 evolution in N_2]	~0[c] [H_2 evolution in N_2]	~0 [H_2 evolution in N_2]	~0 [H_2 evolution in N_2]

[a] Electrode potentials based on Figs. 6 and 7.
[b] Electrode potentials in parenthesis for O_2 reduction in O_2 at ~20 mA cm^{-2}; this potential for Pt|Nafion in H_2CrO_4 is more negative than 0 V vs. SHE at the current density.
[c] Electrode potentials for H_2 evolution in N_2 based on Fig. 2 and the current density in H_2SO_4 is ~3-fold of that in H_2CrO_4 at 0 V vs. SHE (for Pt–C|Nafion); the current density in H_2SO_4 is ~8-fold of that in H_2CrO_4 at −200 V vs. SHE based on Fig. 5 (for Pt|Nafion).

Keeping the cathode potential near what is required for oxygen reduction should not allow impurities such as Cu, Ni, and Fe to be plated out and hydrogen evolution will not occur because the standard electrode potentials for those reactions are much more negative than that required for oxygen reduction on the Pt electrode (Table 1). Unfortunately, this is only true for potentiostatic control in a normally operating MEA in H_2SO_4 (somewhat like the case of Pt–C|Nafion in this work). In normally controlled-current operation in H_2CrO_4, the potential within the MEA can become negative enough to allow deposition of Ni and Fe, though perhaps not Cu.

3.4. Deposition of Cu(II) on the cathode in sulfuric and chromic acid collecting solutions

It is important to determine if the contaminants in the plating baths (e.g. Cu(II)) deposit on the Pt particles inside the MEA, which may increase ohmic resistance resulting in an increasing cell voltage. A planar Pt working electrode and two mixed solutions: 0.1 M $CuSO_4$ in 2 M H_2SO_4; 0.1 M $CuSO_4$ in 2 M CrO_3 were used for cyclic voltammetric experiments to investigate this possibility. The sweeps of CV started from, and ended at, a negative potential.

In these experiments, no Cu oxidation and reduction peaks were detected in the chromic acid solution experiment indicating Cu(II) reduction did not occur; however, in the sulfuric acid solution the Cu(II) reduction peak (at approximate −250 mV) and Cu oxidation peak (around +250 mV) were significant (Fig. 8). A deposit of Cu on the Pt working electrode was visible when the sulfuric acid solution was used but a deposit was not observed when the chromic acid solution was used.

These results were similar to those reported by Goeringer et al. [27] who indicated that a Cu electrode could easily be oxidized by dichromate in a 0.2 M sulfuric acid solution when protons were adequately supplied. This is in contrast to an inference from Ahmed et al. [4,10] that

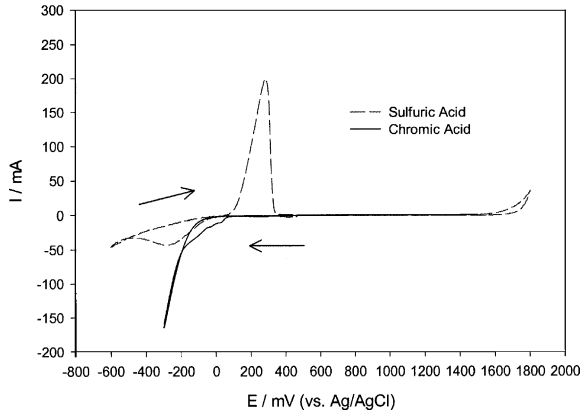

Fig. 8. CVs of Cu(II) on a planar Pt electrode (1 cm^2) for 0.1 M $CuSO_4$ in 2 M sulfuric acid solution and 0.1 M $CuSO_4$ in 2.12 M chromic acid solution. Scan rate = 50 mV s^{-1}.

Cu might be deposited on the Pt catalyst in their Pt–C and contributed to deactivation of the catalyst. The results of our experiments indirectly revealed that the deposition of Cu on Pt particles in the MEAs would be difficult if the catholyte was chromic acid and the cathode was either a Pt|Nafion or Pt–C|Nafion MEA. This could actually be an advantage of using chromic acid versus sulfuric acid, since Cu does not contribute to deactivation of the catalyst.

4. Conclusions

Oxygen reduction was observed on both the Pt|Nafion and Pt–C|Nafion electrodes in both sulfuric and chromic acid solutions when the nitrogen feed gas was replaced by air/oxygen. For the Pt–C|Nafion MEA at high overpotential, the pure oxygen-fed case obtained a greater cathodic current in the sulfuric acid than did the air-fed case, although this did not appear to the case in the chromic acid. By comparing potentials in the high current density regions of the CV diagrams, the active area in the Pt|Nafion electrode appeared to be about an order of magnitude smaller than that in the Pt–C|Nafion electrode.

The oxygen reduction reaction on both electrodes in sulfuric acid resulted in two-slope Tafel plots with a slope of approximately $-120\,\mathrm{mV\,decade^{-1}}$ and a three times higher slope in the high and low current density regions, respectively; however, the Tafel slope for the Pt–C|Nafion electrode was around $-60\,\mathrm{mV\,decade^{-1}}$ in a wider high current density region. In chromic acid, the Pt–C|Nafion electrode also had a Tafel slope close to $-120\,\mathrm{mV\,decade^{-1}}$ in $\log(i) = -3$ to -2 (-600 to 400 mV versus Ag/AgCl) while the Pt|Nafion electrode did not show a clear Tafel region in that range.

The two electrodes obviously gained less cathodic current from oxygen reduction in the chromic acid solution than in the sulfuric acid solution. Therefore, sulfuric acid seems to be a more suitable catholyte than chromic acid for bath regeneration. On the other hand, impurities (i.e., Cu) were more difficult to deposit on Pt in the chromic acid than in the sulfuric acid, which would possibly contribute to deactivation of the catalyst. In addition, the two MEAs had exchange current densities close to $10^{-5}\,\mathrm{A\,cm^{-2}}$ at pseudo-steady-state (scan rate = $1\,\mathrm{mV\,s^{-1}}$) indicating good oxygen reduction kinetics in the electrolytes. Hydrogen evolution was found to be as expected in each electrolyte because of its fast kinetics and the abundance of protons. The results imply that in practical operations, flooding, if it occurs, will be more responsible than oxygen reduction kinetics for the cathodic potential/cell voltage increase in the fuel cell cathode system using chromic acid. Although the Pt|Nafion was easier to flood than the Pt–C|Nafion, the gradual flooding problems during operation will be less serious for the former cathode than for the latter due to a greater porosity in the Pt–C|Nafion than in the Pt|Nafion. In addition, the actual removal of the accumulated contaminants must be accomplished by a process modification, not by deposition on the fuel cell cathode, since the accumulation or recovery of Cu and other contaminants is a necessary feature of the proposed process.

Acknowledgments

The authors would like to acknowledge the help of Professor Khalili at IIT and Professor Der Tau Chin at Clarkson University. Although the research described in this article has been funded in part by the United States Environmental Protection Agency through grant R827125 it has not been subjected to the Agency's required peer and policy review and therefore does not necessarily reflect the views of the agency and no official endorsement should be inferred.

References

[1] M. Uchida, Y. Aoyama, N. Eda, A. Ohta, J. Electrochem. Soc. 142 (1995) 463–468.
[2] A. Parthasarathy, S. Srinivasan, A.J. Appleby, J. Electrochem. Soc. 139 (1992) 2856–2862.
[3] M.S. Wilson, S. Gottesfeld, J. Appl. Electrochem. 22 (1992) 1–7.
[4] M.I. Ahmed, J.R. Selman, T.M. Holsen, J. Appl. Electrochem. 31 (2001) 1381–1387.
[5] D. Pletcher, F.C. Walsh, Industrial Electrochemistry, 2nd ed., Blackie Academic & Professional, New York, 1993, Chapters 2 and 7.
[6] N.V. Mandich, C.-C. Li, J.R. Selman, Plating and Surface Finishing 84 (1997) 82–90.
[7] K.-L. Huang, T.M. Holsen, T.-C. Chou, J.R. Selman, Environ. Sci. Technol. 37 (2003) 1992–1998.
[8] S.L. Guddati, T.M. Holsen, C.-C. Li, J.R. Selman, N.V. Mandich, J. Appl. Electrochem. 29 (1999) 1129–1132.
[9] K.-L. Huang, T.M. Holsen, T.-C. Chou, M.-C. Yang, Environ. Technol. 25 (2004) 39–49.
[10] M.I. Ahmed, T.M. Holsen, J.R. Selman, J. Appl. Electrochem. 31 (2001) 1389–1394.
[11] P.S. Fedkiw, W.-H. Her, J. Electrochem. Soc. 136 (1989) 899–900.
[12] R. Liu, P.S. Fedkiw, J. Electrochem. Soc. 139 (1992) 3514–3520.
[13] P. Millet, R. Durand, E. Dartyge, G. Tourillon, A. Fontaine, J. Electrochem. Soc. 140 (1993) 1373–1379.
[14] P. Millet, A. Michas, R. Durand, J. Appl. Electrochem. 26 (1996) 933–937.
[15] E. Yeager, Electrochim. Acta 29 (1984) 1527–1537.
[16] L.D. Burke, J.K. Casey, J.A. Morrissey, J.F. O'sullivan, J. Appl. Electrochem. 24 (1994) 30–37.
[17] W.-J. Liu, B.-L. Wu, C.-S. Cha, J. Electroanal. Chem. 476 (1999) 101–108.
[18] V.I. Basura, P.D. Beattie, S. Holdcroft, J. Electroanal. Chem. 458 (1998) 1–5.
[19] A. Damjanovic, P.G. Hudson, J. Electrochem. Soc. 135 (1988) 2269–2272.
[20] D.B. Sepa, M.V. Vojnovic, L.M. Vracar, A. Damjanovic, Electrochim. Acta 32 (1987) 129–134.
[21] A. Parthasarathy, C.R. Martin, S. Srinivasan, J. Electrochem. Soc. 138 (1991) 916–921.

[22] A. Parthasarathy, S. Srinivasan, A.J. Appleby, J. Electroanal. Chem. 339 (1992) 101–121.
[23] O. Antoine, Y. Bulyel, R. Durand, J. Electroanal. Chem. 499 (2001) 85–94.
[24] E.A. Ticianelli, E.R. Gonzalez, Fundamental kinetics/transport processes in MEAs, in: W. Vielstich, A. Lamm, H.A. Gasteiger (Eds.), Handbook of Fuel Cells: Fundamentals Technology and Application, vol. 2, Wiley, England, 2003, pp. 493–496.
[25] J.P. Hoare, J. Electrochem. Soc. 126 (1979) 190–199.
[26] S.P. Jiang, J. Appl. Electrochem. 31 (2001) 181–192.
[27] S. Goeringer, N.R. de Tacco, C.R. Chenthamarakshan, K. Rajeshwar, J. Appl. Electrochem. 30 (2000) 891–897.